CHEMICAL ENGINEERING TRANSACTIONS
VOL. 96, 2022
A publication of AIDIC
The Italian Association of Chemical Engineering
Online at www.cetjournal.it
Guest Editors: David Bogle, Flavio Manenti, Piero Salatino

ISBN 978-88-95608-95-2; **ISSN** 2283-9216
DOI: 10.3303/CET2296023

A Bi-objective Optimization Study of an Acid-Base Flow Battery for High Efficiency and Improved Power Density

Andrea Culcasi[a], Luigi Gurreri[a], Alessandro Tamburini[a,*], Ian David Lockhart Bogle[b], Giorgio Micale[a]

[a]Dipartimento di Ingegneria, Università degli Studi di Palermo, Viale delle Scienze Ed.6, 90128, Palermo, Italy
[b]Centre for Process Systems Engineering, Department of Chemical Engineering, University College London (UCL), Torrington Place, London, WC1E7JE, United Kingdom
alessandro.tamburini@unipa.it

Electrical energy storage is critical for a broader penetration of renewable energies with intermittent nature, such as solar and wind energy. The Acid/Base Flow Battery (AB-FB) is a unique, sustainable, and environmental-friendly storage technology with high electrolyte solution energy density. The method relies on reversible electrodialytic technologies using bipolar membranes to transform electrical energy into chemical energy related to pH gradients and vice versa. The charge phase is accomplished by using bipolar membrane electrodialysis, whereas the discharge phase is performed via bipolar membrane reverse electrodialysis. In a previous work, we developed an advanced multi-scale process model (Culcasi et al., 2021b), revealing the importance of operating conditions and design features for the AB-FB battery performance. For the first time, the current work attempts to optimize the AB-FB. The net Round Trip Efficiency and average net discharge power density were maximized in a two-objective optimization. The ε-constraint method was used to construct curves of Pareto optimal solutions under various scenarios, thereby systematically assessing the effect of decision variables consisting of operating and design parameters. The gPROMS Model Builder® software package's optimization tool was used. This optimization study demonstrated that in a closed-loop configuration, optimized operating conditions and design features can be chosen to maximize net Round Trip Efficiency up to 64% and average net discharge power density up to 19.5 W m^{-2} using current commercial membranes.

1. Introduction

Recently, the demand for renewable energy has increased (Culcasi et al., 2021b). However, there is a discrepancy between supply and demand, especially for energy from intermittent sources such as solar and wind. As a result, large-capacity storage systems must be developed, ranging in scale from kWh to MWh. Effective solutions must be scalable, safe, ecologically friendly, durable, cost-effective, and site independent. Importantly, there are various potential methods for energy storage; for example, flow batteries store energy in an electrolyte solution. Acid-Base flow batteries (AB-FBs) are a novel storage method that meet all the above requirements, work well with modern smart grids, and have a high performance (Culcasi et al., 2020). The working mechanism of AB-FB involves with the water dissociation reaction in the bipolar membranes (Culcasi et al., 2021b). Additionally, the AB-FB combines two membrane processes known as Bipolar Membrane Electrodialysis (BMED) and Bipolar Membrane Reverse Electrodialysis (BMRED) (Culcasi et al., 2021a). Specifically, during the charge phase, the externally supplied electricity is transformed into acidic and alkaline solutions, accumulating energy in the form of a pH gradient (Culcasi et al., 2022). During the battery discharge phase, the acid and base streams are neutralised to produce energy. The AB-FB contains repeating units known as triplets, consisting of one anion- and one cation-exchange membrane (i.e., AEM and CEM, respectively), as well as one bipolar membrane (i.e., BPM); all the membranes are separated by net spacers. BPM is made up of two stacked cation and anion exchange layers. In the charge phase, by applying an electrical potential across the AB-FB unit, water dissociation occurs in the interlayer of BPM, resulting in the production of both protons and hydroxide ions (van Egmond et al., 2018) (Figure 1).

Paper Received: 8 February 2022; Revised: 24 July 2022; Accepted: 11 September 2022
Please cite this article as: Culcasi A., Gurreri L., Tamburini A., Bogle I.D.L., Micale G., 2022, A Bi-objective Optimization Study of an Acid-base Flow Battery for High Efficiency and Improved Power Density, Chemical Engineering Transactions, 96, 133-138 DOI:10.3303/CET2296023

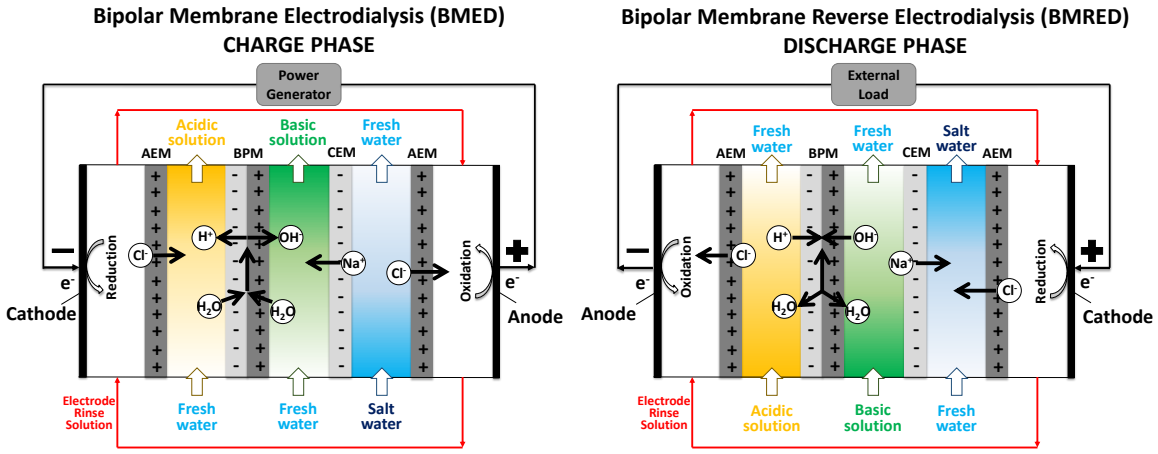

Figure 1. Acid/Base Flow Battery charge a) and discharge b) phases.

When using acid and base solutions at 1 M, it is theoretically possible to achieve a potential energy density of 22 kWh m^{-3} of one solution. Furthermore, higher concentrations of acid and base could still be used to increase the energy density. Notably, the percentage of this energy density recovered varies with the efficiency of the battery charge and discharge phases. Many studies have been carried out in recent years focusing on BMED (Herrero-Gonzalez et al., 2020) (i.e., the AB-FB charge phase), while only a few have been devoted to BMRED (Zaffora et al., 2020) (i.e., the AB-FB discharge phase). In most of these papers, experimental assessments have been conducted under various operating parameters, such as differing electric current or flow rates, and using variable stack dimensions, such as spacer sizes or triplet numbers. These investigations, in particular, found links between the variation of a process variable or a design parameter and the unit performance. Despite the existence of correlations between the numerous process variables, none of the experimental studies could establish a set of parameters that maximise the performance of both the BMED and BMRED processes. In this regard, an AB-FB predictive mathematical tool is a more effective and efficient method to identify the optimal process conditions. However, only a few works in the literature have been focused on the modelling the AB-FB. Moreover, none of these papers has included an optimisation study on either BMED or BMRED so far. Existing optimisation research have been focused on conventional electrodialysis (Rohman and Aziz, 2021) and reverse electrodialysis processes (Long et al., 2018) only. Past single-objective and multi-objective optimisation studies have used the final product concentration, energy consumption, and costs as the objective functions for conventional electrodialysis, and these studies were carried out using a variety of methodologies. For example, the optimisation strategies adopted have included Multi-Objective Genetic Algorithm (MOGA) method (Chindapan et al., 2013), Particle Swarm Optimization (PSO) (Wright et al., 2018), and Response Surface Methodology (RSM) (Guesmi et al., 2020). In conventional reverse electrodialysis, the objective functions are mainly net power density and energy efficiency, and methods such as the genetic algorithm (Long et al., 2018) or the gradient ascent algorithm (Ciofalo et al., 2019) have been used. The AB-FB must be optimised in order to boost the battery competitiveness. Different combinations of operating and design characteristics considerably affect the performance of the unit during both phases (i.e., charge and discharge), and these settings may potentially have opposing effects on performance. The Round Trip Efficiency and average net discharge power density are the primary performance indicators of an AB-FB. Furthermore, pumping power may be relevant in terms of energy consumption, particularly during the discharge phase, when maximising the energy delivery is critical. As a result, power losses must be minimised. A previously validated AB-FB multi-scale model (Culcasi et al., 2021b) was employed in this work to carry out a bi-objective optimisation study of the system. Up to eight operating and design decision variables were simultaneously varied in order to maximise the net Round Trip Efficiency and the average net discharge power density.

2. Method

The operation of the AB-FB is influenced by a variety of detrimental phenomena which must be suitably minimised. These include the transport of co-ions due to the non-ideal behaviour of the membranes. The osmotic and electro-osmotic flows are other deleterious phenomena associated with water transport. Another phenomenon is concentration polarisation in the boundary layer, which results in different ion concentrations at the solution-membrane interfaces compared to the bulk concentrations. Furthermore, shunt currents via manifolds have a significant impact on the performance. To accurately predict the energy efficiency of an AB-

FB, the energy required to pump the electrolytic solutions through the battery must be considered, particularly during the battery discharge phase. The model used in this work was developed with a multi-scale structure, specifically with four-dimensional scales. Some scales also include one or more sub-levels that aim to simulate specific battery components. This model requires membrane properties and battery design characteristics as input. In our previous work, we presented this model and experimentally validated it under various operating conditions. A bi-objective optimisation study was carried out in this work in order to maximise the net Round Trip Efficiency (RTE_{net}) and the average net discharge power density (NPD_d). The net quantities accounted for the power consumed in pumping the solutions. The optimisation study was conducted using the gPROMS Model Builder® platform. The objective functions were computed using the following equations:

$$NPD = GPD \pm PPD \tag{1}$$

$$RTE_{net} = \frac{\int_0^{t_d} (GPD_d - PPD_d)\, dt}{\int_0^{t_c} (GPD_c + PPD_c)\, dt} \tag{2}$$

where GPD is the gross power density (W m^{-2}), PPD is the pumping power density (W m^{-2}), t_d and t_c are the discharge and charge time, respectively. The sign $\pm$ in Equation 1 depends on the battery phase, i.e. $+$ for the charge phase and $-$ for the discharge phase.

The objective was to maximise both the average NPD_d and the net RTE, and both these objective functions had to be calculated simultaneously. In addition, a solution that maximises one of the two functions may not maximise the other, and *vice versa*. As a result, this model provides a set of feasible solutions known as the Pareto front rather than one single solution.

The bi-objective optimisation in this study was carried out using a transformation algorithm known as the ***ε-constraint*** method. This method entails converting the multi-objective problem into a series of single-objective optimisations. Every single-objective problem corresponds to a different point on the Pareto curve. Furthermore, each objective problem involves maximising one of the two objective functions (in this case, the RTE) while constraining the second objective function (i.e., average NPD_d) at a fixed value.

As a result, the following equations can be used to describe the problem:

Objective: $Max\ RTE_{net}(\boldsymbol{x})$ (3)

Subject to: $Av.NPD_d(\boldsymbol{x}) \geq \varepsilon$ (4)

where $\boldsymbol{x}$ is the decision variables vector and ε is the constraint used to obtain the Pareto front. Equation 4 is essential to transform the multi-objective problem into a series of single-objective optimisations.

The battery was simulated in a closed-loop configuration, with each external tank simulated as having perfect mixing. The battery charge and discharge phases were operated until a specific target concentration of HCl in the acid tank was reached, referred to as $C_{target,c}$ and $C_{target,d}$ for charging and discharging, respectively. The decision variables of the optimization study are shown in Table 1, along with their respective lower and upper bounds.

Table 1. List of the decision variables used in the optimization study.

Operating variables				
variable name	scenario	symbol	lower bound	upper bound
charge current density	A,B	i_c	30 A m^{-2}	500 A m^{-2}
discharge current density	A,B	i_d	30 A m^{-2}	200 A m^{-2}
charge mean flow velocity	A,B	$u_{ch,c}$	0.5 cm s^{-1}	5 cm s^{-1}
discharge mean flow velocity	A,B	$u_{ch,d}$	0.5 cm s^{-1}	5 cm s^{-1}
charge target concentration	B	$C_{target,c}$	500 mol m^{-3}	1000 mol m^{-3}
discharge target concentration	B	$C_{target,d}$	50 mol m^{-3}	200 mol m^{-3}
Design variables				
spacer length	B	L	5 cm	200 cm
spacer thickness	B	b	50 µm	1000 µm

Two scenarios were studied in this work, which differed in their number of decision parameters. Specifically, the Pareto curves are illustrated in the case of four (scenario A) and eight (scenario B) decision parameters. Current densities and average mean flow velocities in the channels were used as decision variables in both the charge and discharge phases in Scenario A. Scenario B included, in addition to the decision variables mentioned for Scenario A, the target concentrations of HCl for both the charge and discharge phases, as well as the length and thickness of the spacer.

The optimization study was performed for a single battery cycle. Additionally, for these simulations, the AB-FB reference design developed as part of the European project BAoBaB (Pärnamäe et al., 2020) was used, whose sizes are shown in Table 2. This design minimises battery-detrimental phenomena, particularly shunt currents. This reference design comprises a pile of eight stacks, each containing seven triplets. Since each stack represents a repetitive unit, only one stack was simulated, and the results are representative of the entire pile. The charge transfer reactions, the electromotive force of the electrode reactions, and the ohmic resistances of the end-membrane and electrolyte solutions were simulated as a lumped parameter called blank resistance, which was purposefully measured experimentally at the electrodes.

Table 2. Multi-scale model input for the optimization study adapted from (Culcasi et al., 2021b).

Membrane properties						
	units	AEM	CEM	AEL	CEL	BPM
Thickness	μm	75	75	60	60	120
Areal resistance	Ω cm^2	4.0	3.5	2.5	2.5	5.0
Water permeability	ml bar^{-1} h^{-1} m^{-2}	8	8	-	-	-
H+ diffusivity	m^2 s^{-1}	2.0×10^{-11}	0.7×10^{-11}	2.0×10^{-11}	0.7×10^{-11}	-
Na+ diffusivity	m^2 s^{-1}	1.6×10^{-11}	0.5×10^{-11}	1.6×10^{-11}	0.5×10^{-11}	-
OH- diffusivity	m^2 s^{-1}	1.9×10^{-11}	0.6×10^{-11}	1.9×10^{-11}	0.6×10^{-11}	-
Cl- diffusivity	m^2 s^{-1}	1.7×10^{-11}	0.6×10^{-11}	1.7×10^{-11}	0.6×10^{-11}	-
Fixed charge group	mol m^{-3}	5,000	5,000	5,000	5,000	-
Design parameters						
	units	reference				
Number of triplets	-	7				
Spacer length, L	m	0.44				
Spacer width, b	m	0.476				
Spacer thickness, H	μm	475				
Manifold area	mm^2	400				
Operating conditions at the beginning of the charge						
HCl concentration in the acid tank	mol m^{-3}	50				
NaCl concentration in the acid tank	mol m^{-3}	250				
HCl concentration in the salt tank	mol m^{-3}	10				
NaCl concentration in the salt tank	mol m^{-3}	250				
NaOH concentration in the base tank	mol m^{-3}	50				
NaCl concentration in the base tank	mol m^{-3}	250				
Target concentrations and fluid velocity						
HCl target at the end of the charge	mol m^{-3}	1000				
HCl target at the end of the discharge	mol m^{-3}	50				
Mean flow velocity during charge	cm s^{-1}	1.0				
Mean flow velocity during discharge	cm s^{-1}	1.0				
Electrode compartments and external electric circuit						
Blank resistance	Ω cm^2	12				
Charge current density	A m^{-2}	100				
Discharge current density	A m^{-2}	30				

3. Results and discussion

The first case studied (scenario A) involves the use of four decision variables, namely the current density and mean flow velocity during the charge and discharge phases of the battery (Figure 2).

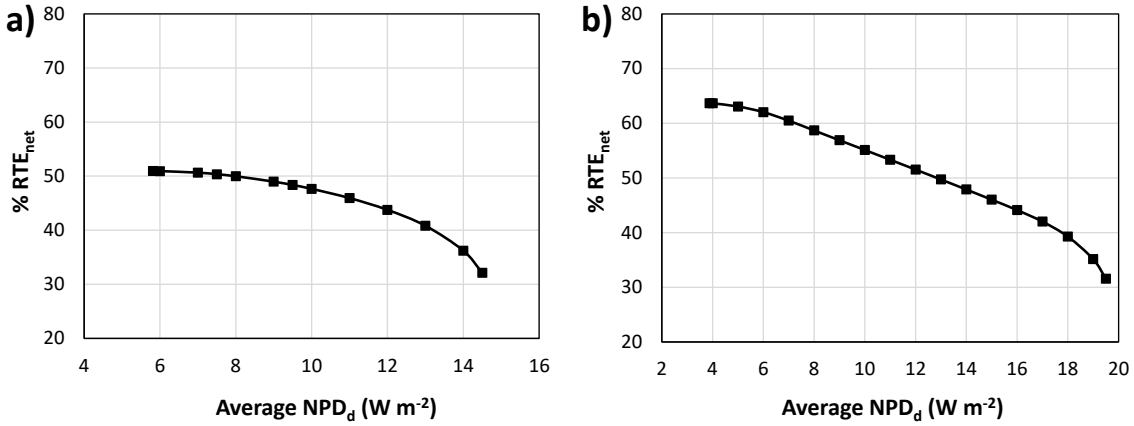

Figure 2. Pareto fronts of net Round Trip Efficiency (RTE_{net}) as a function of the average net discharge power density (NPD_d) in the scenario of a) four decision variables and b) eight decision variables.

As shown in Figure 2a, the Pareto front has a maximum RTE_{net} of 51.0% and an average NPD_d of 5.8 W m^{-2}. As the NPD_d rises, the RTE_{net} shows a decreasing trend. Furthermore, the maximum NPD_d value is 14.5 W m^{-2}, which corresponds to a minimum of 32.1% RTE_{net}. The HCl concentration rises from $C_{target,d}$ to $C_{target,c}$ after the charge phase and the resulting theoretical energy density is 20.1 kWh m^{-3}. Along the Pareto front, this value remains constant because the target concentrations are not included in the decision variables in scenario A. In this case, $C_{target,d}$ and $C_{target,c}$ are equal to 0.05M HCl and 1M HCl, respectively. However, due to non-ideal process phenomena, the energy density obtained during the discharge phase is only a fraction of the theoretical value and depends on the battery discharge efficiency. At the maximum RTE_{net} and average NPD_d, the produced energy densities at the two ends of the Pareto curve are 19.7 kWh m^{-3} and 12.9 kWh m^{-3}, respectively. Indeed, the energy efficiency during discharge is higher, with the value of 97.8%, at maximum RTE, whereas at maximum NPD_d, the efficiency is reduced to 64%. The high energy efficiency of the discharge at maximum RTE_{net} is due to its proximity to open circuit conditions, which increases the electrical efficiency of the discharge phase. Figure 2b depicts the Pareto front for Scenario B, which has eight decision variables. Scenario B, in particular, adds the target concentrations in the two battery phases, as well as two design variables, i.e. the length and width of the spacer, to the four parameters of Scenario A. As the Pareto front shifts upwards, the results show a significant increase in battery performance. Specifically, the maximum RTE_{net} is 64% with an NPD_d of slightly less than 3.9 W m^{-2}, while the maximum NPD_d is 19.5 W m^{-2} with an RTE_{net} of 31.6%. As the scenario target concentrations are decision variables, a variation in the theoretical energy density is observed along the Pareto front. The theoretical energy densities at maximum RTE_{net} and maximum NPD_d are 7.25 kWh m^{-3} and 17.1 kWh m^{-3}, respectively. As a result, higher energy density can be achieved at the expense of lower electrical efficiency. Indeed, similar to the previous Scenario A, at maximum NPD_d, the battery operates at higher charge and discharge current densities than when operating at maximum RTE_{net}, thus reducing energy efficiency. Finally, when maximising the RTE_{net} and NPD_d, the energy efficiencies of the discharge in Scenario B are 87% and ~63%, respectively.

4. Conclusions

A bi-objective optimization study for an Acid/Base Flow battery was performed in this work using a comprehensive multi-scale mathematical model. This study demonstrates how changing the decision variables improves performance in terms of RTE_{net} and average NPD_d. Since the objective functions used have contradictory effects, it is not possible to obtain a single optimal solution, but rather a set of optimal conditions known as the Pareto front. Overall, a maximum RTE of 64% was obtained in a scenario with eight decision parameters and an average NPD_d of 3.9 W m^{-2}, while a maximum average NPD_d of 19.5 W m^{-2} and an RTE_{net} of 31.6% were obtained. This study demonstrates how the appropriate selection of operational and design variables can make this novel battery competitive. This optimization study can be expanded in the future by analysing scenarios with different process configurations and membrane features.

Acknowledgments

This work was performed in the framework of the BAoBaB project (Blue Acid/Base Battery: Storage and recovery of renewable electrical energy by reversible salt water dissociation). The BAoBaB project has received funding from the European Union's Horizon 2020 Research and Innovation program under Grant Agreement no. 731187 (www.baobabproject.eu).

References

Chindapan, N., Sablani, S.S., Chiewchan, N., Devahastin, S., 2013. Modeling and Optimization of Electrodialytic Desalination of Fish Sauce Using Artificial Neural Networks and Genetic Algorithm. Food Bioprocess Technol. 6, 2695–2707. https://doi.org/10.1007/s11947-012-0914-6

Ciofalo, M., La Cerva, M., Di Liberto, M., Gurreri, L., Cipollina, A., Micale, G., 2019. Optimization of net power density in Reverse Electrodialysis. Energy 181, 576–588. https://doi.org/https://doi.org/10.1016/j.energy.2019.05.183

Culcasi, A., Gurreri, L., Cipollina, A., Tamburini, A., Micale, G., 2022. A comprehensive multi-scale model for bipolar membrane electrodialysis (BMED). Chem. Eng. J. 437, 135317. https://doi.org/10.1016/j.cej.2022.135317

Culcasi, A., Gurreri, L., Micale, G., Tamburini, A., 2021a. Bipolar membrane reverse electrodialysis for the sustainable recovery of energy from pH gradients of industrial wastewater: Performance prediction by a validated process model. J. Environ. Manage. 287, 112319. https://doi.org/10.1016/j.jenvman.2021.112319

Culcasi, A., Gurreri, L., Tamburini, A., Cipollina, A., Micale, G., 2021b. Effect of Design Features and Operating Conditions on the Performance of a Bipolar Membrane-Based Acid/Base Flow Battery. Chem. Eng. Trans. 86, 1387–1392. https://doi.org/10.3303/CET2186232

Culcasi, A., Gurreri, L., Zaffora, A., Cosenza, A., Tamburini, A., Micale, G., 2020. On the modelling of an Acid/Base Flow Battery: An innovative electrical energy storage device based on pH and salinity gradients. Appl. Energy 277, 115576. https://doi.org/10.1016/j.apenergy.2020.115576

Guesmi, F., Louati, I., Hannachi, C., Hamrouni, B., 2020. Optimization of boron removal from water by electrodialysis using response surface methodology. Water Sci. Technol. 81, 293–300. https://doi.org/10.2166/wst.2020.105

Herrero-Gonzalez, M., Diaz-Guridi, P., Dominguez-Ramos, A., Irabien, A., Ibañez, R., 2020. Highly concentrated HCl and NaOH from brines using electrodialysis with bipolar membranes. Sep. Purif. Technol. 242, 116785. https://doi.org/10.1016/j.seppur.2020.116785

Long, R., Li, B., Liu, Z., Liu, W., 2018. Performance analysis of reverse electrodialysis stacks: Channel geometry and flow rate optimization. Energy 158, 427–436. https://doi.org/10.1016/j.energy.2018.06.067

Pärnamäe, R., Gurreri, L., Post, J., van Egmond, W.J., Culcasi, A., Saakes, M., Cen, J., Goosen, E., Tamburini, A., Vermaas, D.A., Tedesco, M., 2020. The Acid–Base Flow Battery: Sustainable Energy Storage via Reversible Water Dissociation with Bipolar Membranes. Membranes (Basel). 10, 409. https://doi.org/10.3390/membranes10120409

Rohman, F.S., Aziz, N., 2021. Performance metrics analysis of dynamic multi-objective optimization for energy consumption and productivity improvement in batch electrodialysis. Chem. Eng. Commun. 208, 517–529. https://doi.org/10.1080/00986445.2019.1674817

van Egmond, W.J., Saakes, M., Noor, I., Porada, S., Buisman, C.J.N., Hamelers, H.V.M., 2018. Performance of an environmentally benign acid base flow battery at high energy density. Int. J. Energy Res. 42, 1524–1535. https://doi.org/10.1002/er.3941

Wright, N.C., Shah, S.R., Amrose, S.E., Winter, A.G., 2018. A robust model of brackish water electrodialysis desalination with experimental comparison at different size scales. Desalination 443, 27–43. https://doi.org/10.1016/j.desal.2018.04.018

Zaffora, A., Culcasi, A., Gurreri, L., Cosenza, A., Tamburini, A., Santamaria, M., Micale, G., 2020. Energy Harvesting by Waste Acid/Base Neutralization via Bipolar Membrane Reverse Electrodialysis. Energies 13, 5510. https://doi.org/10.3390/en13205510